East West University

Project Title

Analysis of electromagnetic properties of Graphene Nano-Ribon (GNR)

Submitted by:
Kazi Ashraful Haque
ID: 2011-3-55-005

Project Supervisor:
M. Mofazzal Hossain, Ph.D.
Professor
Department of Electronics and Communication Engineering

Declaration

I hereby declare that I have completed project on the topic entitled "Analysis of electromagnetic properties of Graphene Nano-Ribon(GNR)" as well as prepared as research report to the department of Electronics and Communication Engineering East West university in partial fulfillment of the requirement for the degree of B.Sc. in Electronics and Telecommunication Engineering, Under the course "Research/internship (ETE 498)".

I further assert that this report in question is based on my original exertion having never been produced fully and/or partially anywhere for any requirement.

……

Kazi Ashraful Haque
ID: 2011-3-55-005
Department of ECE
East West University

Acceptance

This research report presented to the department of electronics and communication engineering, East West University is submitted in partial fulfillment of the requirement for degree of B.Sc. in Electronics and Telecommunication Engineering, under complete supervision of the undersigned.

……

M. Mofazzal Hossain, Ph.D.
Professor
Department of Electronics and Communication Engineering

Acknowledgement

First and foremost with all my heartiest devotion I am grateful to almighty Allah for blessing me with such opportunity of learning and ability to successfully complete the task.

A special Thanks with honor to my supervisor Engr M. Mofazzal hossain who was kind enough to allocate his valuable time to provide me with his humble guidance, motivating thought and encouragement.

……
Kazi Ashraful Haque
2011-3-55-005

Abstract

A theoretical investigation is carried out to see the change of electromagnetic Graphene Nano-Ribon with respect to number of layer of its own. To see this change we have consider a electrical circuit of graphene nano-Ribon . There we have seen the effect of it electromagnetic properties. At 1st we have seen the effect of its resistance with respect to its width. Then we have seen the change of its Resistance, inductance and capacitance with respect to number of layer of its own. We also observed the band gap effect of graphene nano-ribon with respect to its width. Graphene Nano-Ribon(GNR) is not yet using widely in the modern world rather this is a future aspect that will surely be used in recent future.

INDEX

Contents **Page No**

Chapter 1

Introduction

Carbon is the most important element for all living organisms on earth, as most of the organic elements are made out of it. The unique and fascinating carbon materials are formed by the carbon atoms bond with each other in various ways, exhibiting linear, planar, and tetrahedral bonding arrangements. Carbon material is an ancient yet vigorous material; in roughly 5000 BC, our ancestors began to utilize charcoal for heating and cooking food (energy materials) and subsequently, they used charcoal to smelt copper and iron (chemical materials). Today, carbon materials have been developed to form a brand of the inorganic nonmetallic material that occupies an important place in materials science. Carbon materials are widely used in various industries from aerospace to chemical to nuclear. They are ubiquitous in our daily lives, where they are used in metallurgy, machinery, automotive, medical, environmental, and construction applications.

Today, carbon materials have been developed to form a brand of the inorganic nonmetallic material that occupies an important place in materials science. Carbon materials are widely used in various industries from aerospace to chemical to nuclear. They are ubiquitous in our daily lives, where they are used in metallurgy, machinery, automotive, medical, environmental, and construction applications.

Graphene Nano ribbons represent a novel class of low-dimensional materials. All these graphene based nanostructures are expected to exhibit the extraordinary electronic properties and therefore these are the promising candidates for a wide range of Nano science and nanotechnology applications. CNT is graphite sheet with a hexagonal lattice that has been wrapped up into a seamless cylinder. GNR consists of carbon atoms arranged in a 2-dimensional honeycomb crystal lattice. And rode like silicon crystals with a diameter of less than 100 nm is referred to as SiNW. These materials are being used as the channel materials of the transistors.

Graphene as a 2-D unit for the construction of graphite was first explored by theoretical research in 1947 as the starting point to understanding the electronic properties in three-dimensional (3-D) graphite. However, it was theoretically predicted almost 80 years ago that strictly 2-D crystals cannot exist because the thermal fluctuation would destroy long-range order, giving rise to the melt of 2-D lattices. Nevertheless, the experimental research of producing 2-D materials, especially graphene, has never been interrupted. Early attempts to isolate graphene sheets from graphite was conducted by using graphite intercalated compounds as the raw materials, since intercalation of heteroatoms of molecules between graphene layers in graphite can effectively reduce the interlayer interaction and expand interlayer distance. Extremely thin graphite lamellae were also prepared starting with graphite oxide, an oxidized state of graphite. It was discovered that ultrathin carbon films could be obtained by heating or by reduction of graphite oxide in alkaline suspension. This paper reported the ultrasmall thickness of 0.4–2 nm for the exfoliated sheets by analyzing the contrast of the samples in transmission electron microscopy (TEM) images corresponding to mono- and few-layer samples. Although it is now known that it is impossible to distinguish the layer numbers of graphene by simply comparing the contrast, and that the graphite oxide-derived samples have large amounts of structural defects and functional groups, this early attempt does shed light on the chemical preparation of graphene.

Graphene is a flat single atomic layer sheet of carbon atoms, which is two-dimensional, and it is packed into a honeycomb lattice, as shown in Figure 1. Previously it was believed that two-dimensional crystals were thermodynamically unstable until single-layer graphene in 2004 was discovered. The stability of the experimentally discovered 2D single-layer grapheme is because of the gentle crumples in the third dimension, which has been proved from the far more investigations. Graphene has been studied as the basic building block for all the graphitic materials for more than sixty years. Because it can be wrapped into 0D bucky balls, rolled into 1D carbon nanotubes (CNT), or arranged in sheets to form 3D graphite. The discovery of single layer graphene has led to a revolution in the research field of condensed matter physics. The exceptional electronic characteristics are the main reason of it. Excellent electronic and thermal characteristics can be seen in Graphene and it is very much similar to those of carbon nanotubes (CNT) . Graphene is immune to electromigration, which causes problems in copper interconnects beyond the 130 nm technology node. Graphene has the capability of sustaining current densities up to three orders of magnitude higher than that of typical copper interconnects. electrons can travel long distances in grapheme without being scattered because of a certain electronic characteristics.

In this work, We have analyzed Graphene Nano-Ribon in an electrical circuit model . And we have seen the effect of Graphene in terms of its Width and number of layer for its electrical properties. We have found some interesting effect for this. There is a good effect for width for the resistance. We have seen the effect in term of width for the Resistance. And also we have seen the effect on resistance, inductance and capacitance in term of the number of layer of Graphene. Also we have seen the Band Gap relation with width. With the change of width how bang gap increase or decrease, we found that through this research.

References

[1] Yijian Ouyang, Youngki Yoon, and Jing Guo, "Scaling Behaviors of Graphene Nanoribbon FETs: A Three Dimensional Quantum Simulation Study",IEEE Transactions on Electron Devices, Vol. 54, pp. 2223-2231, September 2007.

[2] Y. Ouyang, Y. Yoon, J. K. Fodor, and J. Guo, "Comparison of performance limits for carbon nanoribbon and carbon nanotube transistors", Applied Physics Letters, vol. 89, pp. 203107.1-203107.3, 2006.

[3]. Debe, M. K. 2012. Electrocatalyst approaches and challenges for automotive fuel cells. *Nature* 486(7401):43–51.

[4] Antolini, E. 2009. Carbon supports for low-temperature fuel cell catalysts. *Appl. Catal.* Graphene

[5] Sharma, S. and Pollet, B. G. 2012. Support materials for PEMFC and DMFC electrocatalysts—a review. *J. Power Sources* 208:96–119.

[6] Wang, Y.-J., Wilkinson, D. P. and Zhang, J. 2011. Noncarbon support materials for polymer electrolyte membrane fuel cell electrocatalysts. *Chem. Rev.* 111(12):7625–7651.

[7] Antolini, E. 2012. Graphene as a new carbon support for low-temperature fuel cell catalysts. *Appl. Catal. B* 123:52–68.

[8] Geim, A. K. and Novoselov, K. S. 2007. The rise of graphene. *Nat. Mater.* 6(3):183–191.

[9] Chen, D., Tang, L. and Li, J. 2010. Graphene-based materials in electrochemistry. *Chem. Soc. Rev.* 39(8):3157–3180.

Chapter 2

Graphene NanoRibbon (GNR)

2.1 History of GNR

Graphene, it is defined as a monolayer of carbon atoms that are hexagonally tightly packed into a 2-D lattice. The structure of graphene can also be viewed as the fewest layer limits of graphite, and graphene can be produced from graphite by complete exfoliation of graphite into monoatomic layers. Graphite as a traditional carbon material has been widely used in our daily lives for centuries. Layered structure is one of the typical characteristics of graphite, which has been successfully utilized in many applications, including the pencil lead for writing, the most universally familiar application of graphite. When you write using a pencil, thin graphite flakes are delaminated from the lead by the mechanical friction between graphite in the pencil lead and paper.

Graphene was fisrt explored as a 2-D unit for the construction of graphite in 1947 by theoretical research. It was the starting point to understanding the electronic properties in three-dimensional (3-D) graphite. Almost 80 years ago there were a theoretically prediction that strictly 2_D crystal cannot exist because the thermal fluctuation would destroy long-range order, giving rise to the melt of 2-D lattices. The experimental research of producing 2-D material more over Graphene has been interrupted. Early attempt to isolate grapheme sheets from graphite was conducted by using ghraphite intercalated compounds as the raw materails, since intercalation of heteroatom of molecules between Graphene layers in graphite can effective reduce the interaction. It also expand interlayer distance. Thin graphite were also prepared starting with graphite oxide in an oxidized sate of graphite. It was discovered that ultrathin carbon films could be obtained by heating or by reduction of graphite oxide in alkaline suspension. The reference paper reported the ultra-small thickness of 0.4-2nm for exfoliated sheets by analyzing the contrast of the samples in transmission electron microscopy (TEM) images corresponding to mono- and few-layer samples [1]. Now a days it is known that the graphite oxide-derived samples have large amounts of structural defects and functional groups. And also it is seems to be impossible to distinguish the layer number of graphene. And that is the early attempt does shed light on the chemical preparation of Graphene.

In the past few decades, Single- or few-layer graphene has been epitaxially grown using gaseous carbonaceous precursors on certain substrates or thermal ecome attached the paper to form writing traces. There is no doubt that monoatomic layer delamination can occur during this process though the possibility may be extremely low. Therefore, it can be speculated that graphene may have already been produced centuries ago by anyone who used a pencil to write or draw, but it has never been realized and taken into serious consideration until the twentieth century. Decomposition of silicon carbide (SiC) and it has high crystallinity and high

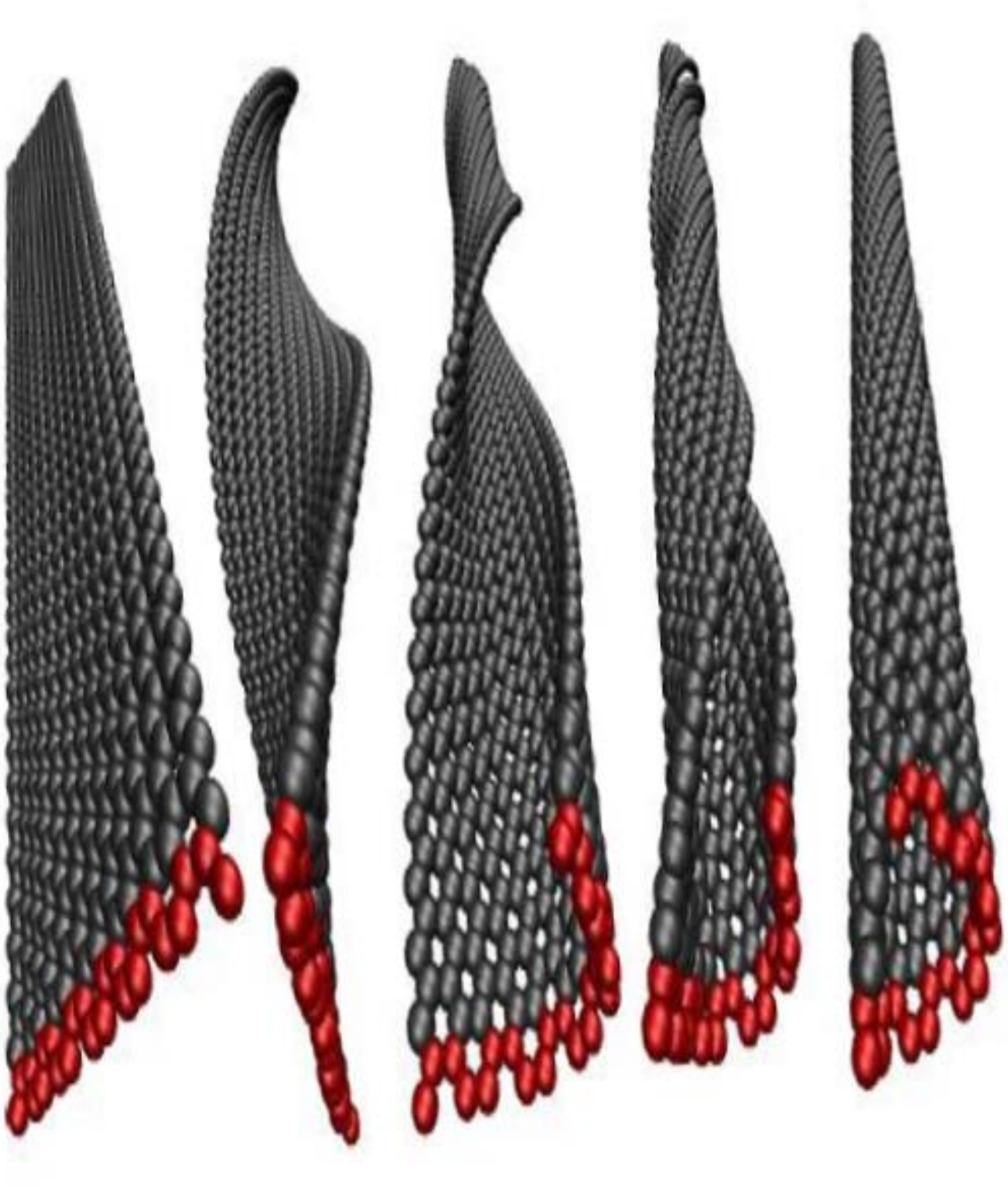

Figure (2.1): Graphene Nano-Ribbon (GNR)

Mobility charge carriers[3]. There is strong interaction between graphene and the substrate which significantly alters the electronics structure of graphene. And for this reason, the measured

electronic properties of graphene on the subsrates may not truly reflect the properties of intrinsic graphene in a free-standing state.

Until the 2004 publication of pioneering work of Geim, Novoselov, and their research group that the curtain of the broad stage for this magic carbon material was finally drawn. Their experiment were quite simple. Its principle of the experiment is the mechanical exfoliation of graphite, which is actually analogous to the writing on a paper using a pencil but in a more controllable way. By repeating cleavage of graphite using common Scotch tape, the exfoliation process was realized. Ultrathin graphene sheets were finally produced with great patience. One of the secrets to their success is the usage of a silicon (Si) wafer with a 300-nm-thick silicon dioxide (SiO2) layer on top as the substrate to load exfoliated thin graphite flakes. Such a substrate makes it possible to distinguish ultrathin graphitic layers simply by using optical observation, which enormously enhances the efficiency of the search for graphene. The as-prepared graphene is perfect in structure with almost no defects, and therefore it is possible to experimentally measure the intrinsic properties of graphene for the first time. The unique electronic properties of graphene astonished scientists, and soon significant attention was focused on this magic new carbon material all over the world. Due to their remarkable and pioneering research work, the Nobel Prize in Physics 2010 was jointly awarded to Geim and Novoselov for "groundbreaking experiments regarding the two dimensional material graphene"[3]. Till today, tens of thousands of research papers have been published and also thousands of patents have been applied based on the materials and techniques related to graphene. It is believed that graphene may become a revolutionary new material that will change the world in the near future with its special effect.

2.2 **Types of GNR**

There are two types of Graphene Nano-Ribon : armchair, zig-zag. The names armchair and zigzag named after their characteristic appearance on the atomic scale and follow the standard GNR literature convention, which is opposite to the CNT (carbon nanotube) convention.

2.1.1 Zig-zag GNR

The edge sites are emphasized by solid circles on each side. Perpendicular to the direction of defined width, GNRs repeat their geometric structures, and form one-dimensional periodic structures. Since GNRs are stripes of graphene, edge atoms are not saturated. Therefore, active edge states become an important factor to determine the edge structures. For zigzag GNRs, it was unexpectedly found that the zigzag edge is metastable, and reconstruction spontaneously takes place at high temperature. The width of zigzag GNR plays an important role. The electronic properties of zigzag graphene nanoribbons (Z-GNRs) adsorbed on Si substrate strongly depend on

ribbon width.

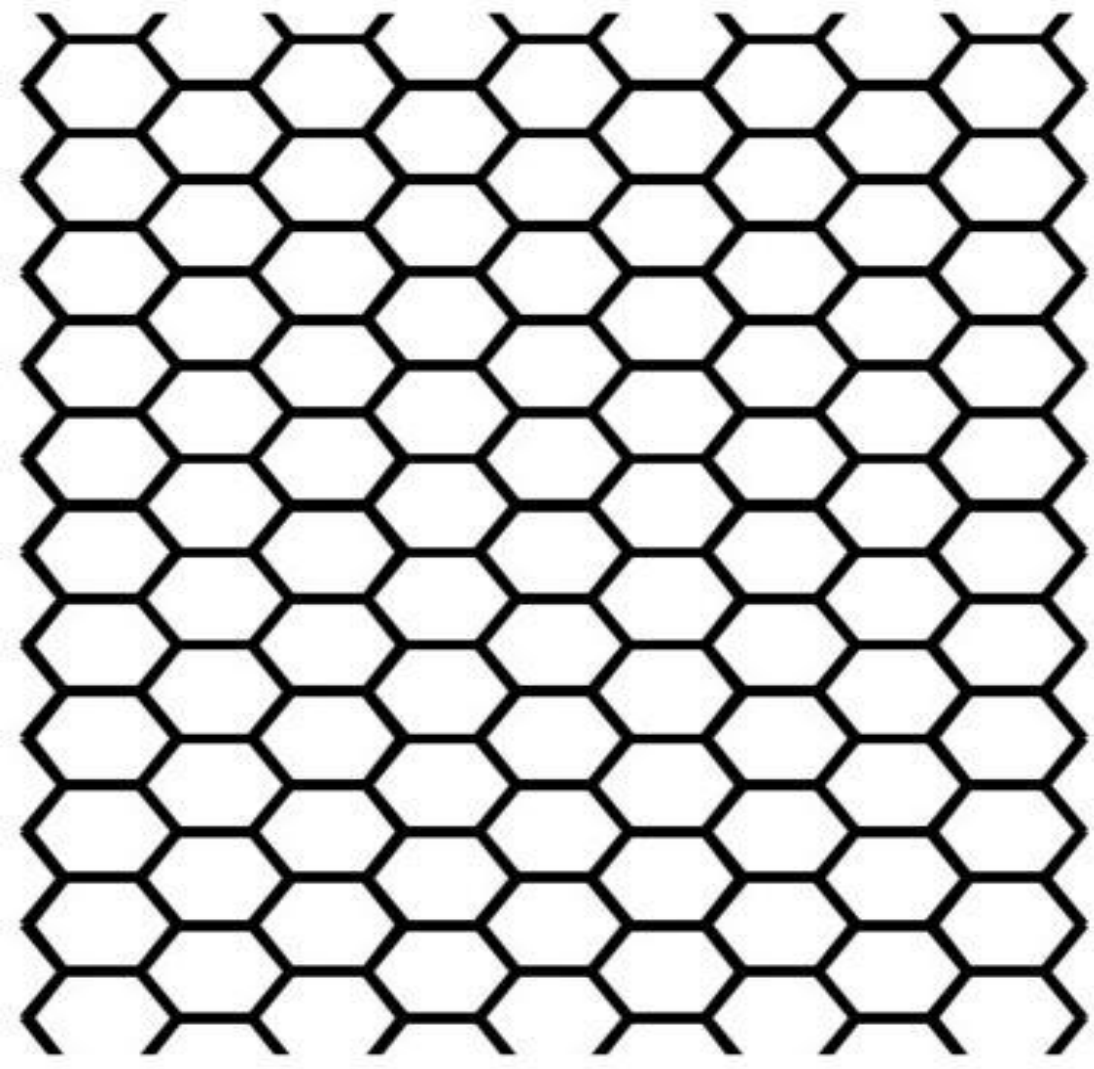

Fig(2.2): Zig-zag Graphene Nano-Ribon

The width of a zigzag ribbon is now identified with the number of zigzag chains N [19],
Wzz= (N-1)(^{3}/2)a With a = 1.42Å nearest neighbor distance

2.1.1.1Electron Transport in Zigzag GNR

From monolayer graphene, graphene nanoribbon (GNR) with a finite width has been shown to hold unusual electronic properties depending on their edge shape and width. Depending on these earlier studies all zigzag GNRs (ZGNRs) were predicted to be metallic, while AGNRs were grouped into semiconducting and metallic character. The metallic character of ZGNRs was

attributed to the presence of a high density of edge states at the Fermi level. The zigzag edges present electronic localized states at the boundaries, corresponding to non-bonding states that appear at the Fermi level as a large peak in the density of states. Phenomena related to magnetic and spin properties arising due to specific edge structure of graphene ribbons have also been investigated theoretically. Due to the non-bonding character of the zigzag localized edge states, the geometrical reconstruction is unlikely to happen and the spin polarization of the electronic density establishes an anti-ferromagnetic arrangement (Figure 2.3) with the opening of a gap, yielding a Slater insulator [4] .

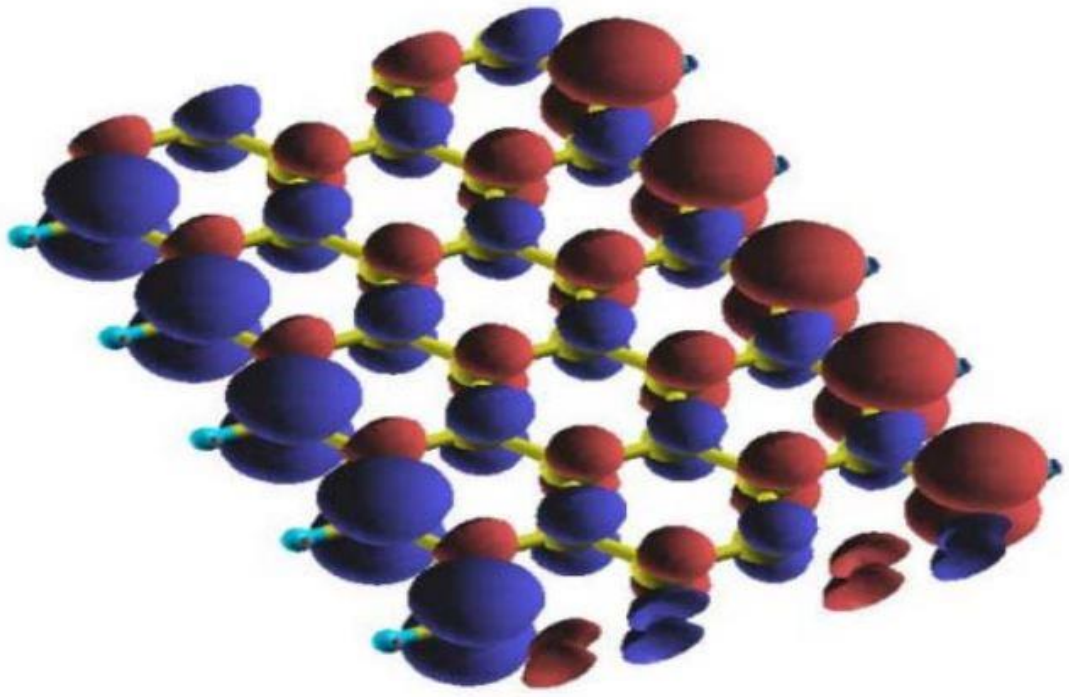

Figure (2.3) : Spin density map, showing the anti-ferromagnetic arrangement between opposite edges(Ricardo F et al., 2009 [20]).

In details, graphene nanoribbons with zigzag edges (ZGNRs) possess spin polarized peculiar edge states and spin polarized electronic state provides half metallicity under transverse electric field and has great potential in the application as spintronics. It is mainly attributed that an in plane electric field, perpendicular to the periodic axis, induces a half metal state in zigzag nanoribbons (ZGNR). Apart from the interesting dependence of the electronic structure upon an electric field, this is a promising material for future spintronic devices, since it could work as a perfect spin filter.

2.1.2 Armchair GNR

The edge sites are emphasized by solid circles on each side. Perpendicular to the direction of defined width, GNRs repeat their geometric structures, and form one-dimensional periodic structures. Since GNRs are stripes of graphene, edge atoms are not saturated. Therefore, active edge states become an important factor to determine the edge structures. For armchair GNRs (figure 2.4), there is no edge reconstruction, and the planar patterns are kept.

Wac=(N-1)((³^.5/2)a With a = 1.42Å nearest neighbor distance

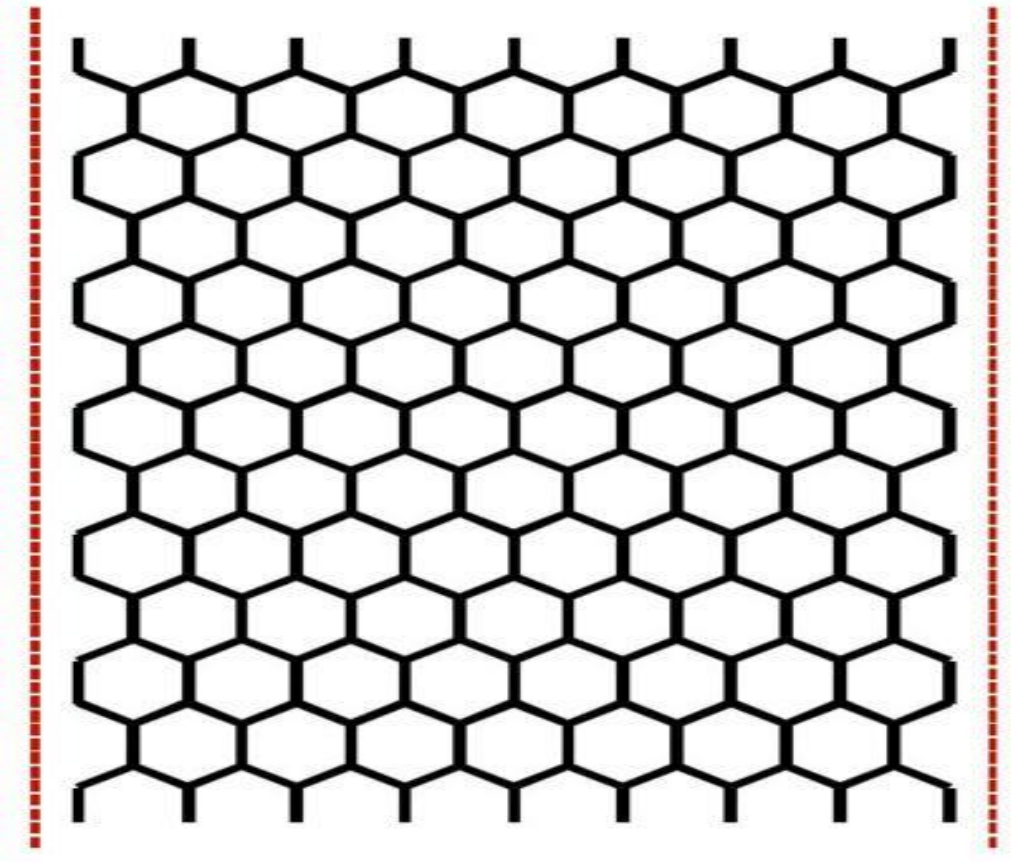

Figure (2.4): Armchair graphene Nano-Ribon

The width of an armchair ribbon can be defined in terms of the number of dimer lines [5]

2.1.2.1 Electron Transport in Armchair GNR

Many theoretical studies have been devoted into investigating the electronic properties of armchair GNRs, such as tight-binding calculations, density functional theory (DFT) calculations, and many-electron green‘s function approach. Among those methods, DFT calculations adopt parameter free

self-consistent field calculations, and their reliability has been broadly proved in solid state field and nano-scale systems. Thus, most of the theoretical investigations have been carried out with DFT calculations. However, it is well established that DFT calculations underestimate band gaps. Other methods, such as tight-binding calculations, have been adapted to correct DFT calculations, and get the reliable band gaps. Armchair GNRs show semiconducting behaviors with a direct energy gap. The determining factor comes from the quantum confinement effect (QCE), which can be characterized by energy gaps is inverse of width. Besides the QCE, researchers have pointed that the edge effects play an important role to force the armchair GNRs to be semiconductors. As shown in figure 2.4, the edge of carbon atoms of armchair GNRs are usually passivated by hydrogen atoms, which lead to the bonding of carbon atoms at the edges different with other carbon atoms. As a consequence, the bond lengths of carbon atoms at the edges are shorter than that in the middle of ribbons, and open the energy gaps of armchair GNRs. Although armchair GNRs have three typical families (corresponding to N = 3p, 3p+1, 3p+2, respectively, where p is any integer) with distinguished energy gaps, they have similar band shapes [6].

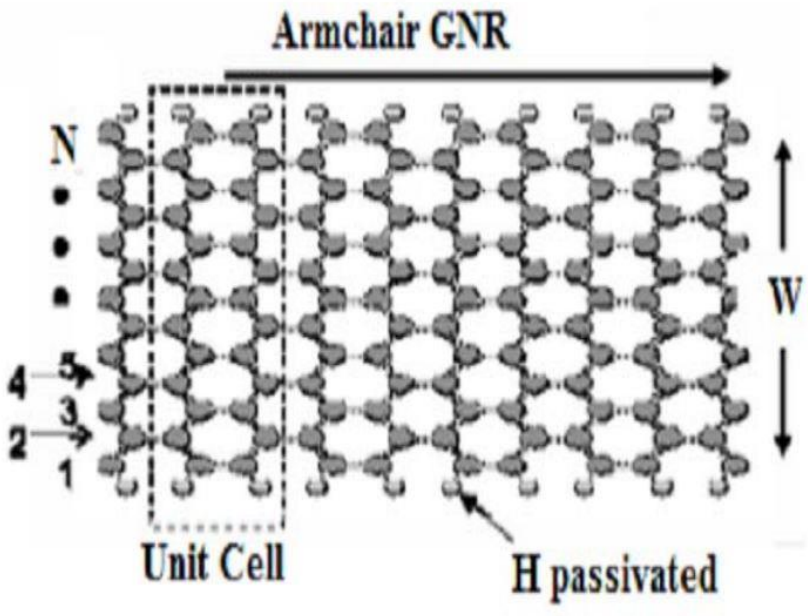

Figure (2.5): Atomic structure of armchair Graphene Nano-Ribon [7]

2.3 **Properties**

Properties of Graphene nano-Ribon are quite different that the material we generally use. These properties made GNRs such important materials for using in Nano technology. Some properties are discussed below in general.

2.3.1 **Electronic properties**

The high quality of 2-D crystal lattice endows graphene with extraordinary electronic properties. The valence and conduction bands in graphene intersect at a single point of zero states, which is called the Dirac point, which makes graphene a zero-gap semiconductor. At the Dirac point, the density of states is zero and the linear dispersion relation results in an effective mass of zero. Therefore, electrons in graphene behave as massless Dirac fermions, giving rise to unprecedentedly high carrier mobility. The carrier mobility measured for a high-quality single-layer graphene sheet prepared by mechanical exfoliation and completely suspended with no influence of the substrate reaches 200,000 cm2 V–1 s–1 [26]. With such high-carrier mobility, the charge transport in graphene is actually ballistic on the micrometer scale at room temperature. The charge carriers in graphene behave like relativistic particles. As a result, their behavior should be described using the Dirac equation instead of the Schrodinger equation, generally applied to describe the electronic properties of other materials. Therefore, the emerge of graphene now provides scientists with the possibility to investigate relativity theory on the lab table instead of in the universe, and provides a way to study quantum electrodynamics by measuring graphene's electronic properties. Another characteristic of graphene is its ambipolar electric field effect. The carriers in graphene can be continuously tuned between holes and electrons by supplying the requisite gate bias. This means that under negative gate bias, the Fermi level drops below the Dirac point, giving rise to a large population of holes in the valence band, while under positive gate bias, the Fermi level was raised above the Dirac point, introducing a large population of electrons in the conduction band. The mobility of charge carriers can exceed 15,000 cm2 V–1 s–1 even when their concentration is as high as 1013 cm–2 at ambient conditions [8,9] and the observed mobility is weakly dependent on temperature. Due to the atomically thin structure of graphene, electron transport on graphene is strictly confined in the 2-D plane, which creates a so-called 2-D electron gas and induces some unique phenomena, such as a quantum Hall effect even observed at room temperature. Klein tunneling is another feature of graphene, which is derived from the chiral nature of electron transport in graphene. This means that the electrons in graphene have a 100% transmission rate through a potential barrier of any size. This may bring about some difficulties in manipulating graphene-based devices, as square potential barriers usually applied to form the device channel may be ineffective for graphene. The intrinsic electronic properties of graphene have been extensively studied and will cause not much excitement on their own. However, the interference of graphene with intrinsic or extrinsic scatters, such as doping atoms or substrates, will cause novel transport phenomena, which is a useful way to tune the electron properties of graphene to meet different application purposes.

2.3.2 Optical properties

About 97.7% of a single layer has been experimentally observed in the visible range for a constant transparency, which means that atomic monolayer graphene has an unexpectedly high opacity, absorbing $\pi\alpha \approx 2.3\%$ of white light, where α is the finestructure constant [10]. This is a consequence of the unusual low-energy electronic structure of monolayer graphene that features electron and hole conical bands meeting each other at the Dirac point. It is noteworthy that the transmittance decreases linearly with the number of layers for multilayer graphene [11], so that the thickness of multilayer graphene with less than 10 layers can be determined using white light illumination on samples supported on a given substrate. However, if the thickness of graphene increases to more than 10 layers, the optical property eventually becomes more like that of graphite. Based on the Slonczewski–Weiss–McClure band model of graphite, the interatomic distance, hopping value, and frequency cancel when optical conductance is calculated using Fresnel equations in the thin-film limit. That is to say, thick graphene platelets with tens of layers will never share the same optical property with the monolayer one.

Considering the real application for a graphene-based Bragg grating, which is a one-dimensional photonic crystal, has been fabricated and demonstrated its capability for excitation of surface electromagnetic waves in the periodic structure by using a 633-nm helium–neon (He–Ne) laser as the light source.

2.3.3 Thermal properties

Single-layer graphene has the highest intrinsic thermal conductivity that has ever been found in any material. As high as 6000 W m–1 K–1 [12], the intrinsic thermal conductivity of graphene is even higher than its allotrope-carbon nanotube, which is 3500 W m–1 K–1 [13,14], and certainly higher than those metals with good thermal performance, such as gold, silver, copper, and aluminum. This excellent thermal performance is born from the unique electronic and topographic features of graphene. However, according to [15], placing graphene on substrates results in serious degradation of thermal conductivity to 600 W mK–1, lower than values obtained for suspended graphene. Since the carrier density of nondoped graphene is relatively low, the electronic contribution to thermal conductivity is negligible according to the Wiedemann–Franz law [16]. The thermal conductivity of graphene is thus dominated by phonon transport, namely diffusive conduction at high temperature and ballistic conduction at sufficiently low temperature. Now we can say that the degradation of thermal conductivity is owing to the phonons leaking across the graphene-support interface and strong interface scattering of flexural modes. In any case, due to the extraordinary thermal conductivity of graphene, graphene functionalized nanocomposites have been studied for various advanced applications including thermal management of advanced electronic chips, thermal pastes, and smart polymers.

2.2.4 Mechanical Properties

Graphene is mechanically strong while remaining very flexible, which is attributed to the high strength of the carbon–carbon bond. The elastic properties and intrinsic breaking strength of free-standing monolayer graphene were measured by nanoindentation using an atomic-force

microscopy [17]. The experimental data showed that the mechanical properties of graphene measured in experiments have exceeded those obtained in any other material, with some reaching theoretically predicted limits that were investigated by numerical simulations such as molecular dynamics [18]. For example, a single-layer, defect-free graphene was measured with a Young's modulus of 1 TPa and intrinsic fracture strength of 130 GPa. These high values make graphene very strong and rigid and these incredible mechanical performances are benefited from the hexagonal structure of graphene. Interestingly, despite sharing the same honeycomb lattice, bulk graphite is not particularly strong because it shears very easily between layers. As a derivative of graphene, GO in a paper form was prepared and studied as a ramification of graphene. The average elastic modulus and the highest fracture strength obtained were about 32 GPa and 120 MPa, respectively [19]. The decrease of Young's modulus may be caused by the defects introduced during the chemical reaction. After reduction with hydrazine or annealing, a paper composed of stacked and overlapped graphene platelets was obtained and the stiffness and tensile strength were reinforced [20]. Chemically modified graphene obtained by reducing GO with hydrogen plasma exhibited a mean elastic modulus of 0.25 TPa with a standard deviation of 0.15 TPa. Just as the Nobel announcement said, a 1-square-meter graphene hammock would support a 4-kg cat, but would weigh only as much as one of the cat's whiskers at 0.77 mg, which is about 0.001% of the weight of 1 m2 of paper. These outstanding intrinsic mechanical properties make graphene suitable for diverse applications such as pressure sensors, resonators, and engineering components subjected to large mechanical stresses even under extreme conditions.

2.2.5 Tailoring the Physical Properties of Graphene

With emphasis on its potential in electronics mechanical devices and photonics the basic properties of Grapheen is described. Adding to that fact, the state of the art regarding other important physical aspects of grapheme beyond its electrical properties is also reviewed including its mechanical, magnetic and thermal properties.

2.2.6 Magnetic Transport Properties of Graphene Nanoribbons

Theoretical investigations are done on spintronics and magnetic device properties of STGNRs. The typical properties of bipolar magnetic semiconductors are featured by the STGNRs at a FM ground state. Compared to ZGNRs their Curie temperature T is much higher. A very significant fact is that the dual spin filtering effect with the perfect spin polarization and high performance dual spin diode effect with a rectification ratio about 10^{10} can be achieved. This is a much greater value as compared to that for a ZGNR diode (~10^5~) and macroscopic p-n junction diodes (10^{5}~ 10^7). A giant magnetoresistace approaching 10^{10}% displayed by a highly effective spin valve device is three orders magnitude higher than the value predicted based on the ZGNRs and six orders magnitude higher than previously reported experimental values for the MgO tunnel junction. These idiosyncratic features can be endorsed to their unique band overlap pattern for two electrodes and particular sensitivity to a switching magnetic field. For developing STDs, the research suggests that STGGNRs have a promising performance.

For edge carbon atoms of GNRs there exists two types of hybridizations, sp^2 and sp^3 hybridizations. The usual edge structure under a lower hydrogen-concentration is generally

regarded as the sp^2 hybridized mono hydrogen termination. That is why, in most of the literatures mono hydrogen terminated structures fog nr are presented and investigated. This type of termination for STGNRs is still being searched. Edge structure of GNR is usually diversified, for example di-hydrogen termination, edge reconstruction, Z, passivate edge, edge defects and other chemical modifications. These might have an impact on magnetism. Further works will deal with this complicated cases. It is quite difficult to achieve the required atomic precision for fabricating StGNRs in the current experiments, but theoretical modeling to understand the magnetic structure and magnetic transport properties of ideal STGNRs is very much significant.

Exchange correlation functionals for DFT used in our works might underestimate the band gap of AGNRs compared with other algorithms. The GW method is one of its example. If other more exact methods are used for calculations there would be a larger spin splitting energy gap E.Spin splitting energy gap is really well related with the spin polarization and spin diode effect as well as the spin valve device.

2.2.7 **Non-Linear properties**

Linear elastic behavior of all GNRs are being displayed from the nominal stress-strain curves in Fig-2. Following that the linear regimes of the GNRs can be written as b e E W E0 E0 0 3 = +, (21).

Here b E0 is the initial young modulus of the bulk grapheme and e E0 is the initial edge modulus. The bulk graphene is isotropic in the regime of linear elasticity and the edge modulus depends on the edge chirality with different values for the zigzag and armchair edges. As it is shown in Fig. 3, the initial Young's modulus of the GNR depends on the edge chirality and the ribbon width. present studies after using the REBO potential express their views that a bulk Young Modulusm 243 0=b E N/mm and the predicted edge modulus is 8.33 0= e E nN (52 eV/nm) for the unpassivated zigzag edge and =3.65 e E nN (~22.8 eV/nm) for the unpassivated armchair edge. The Young mdulus among positive moduli for both edges, the GNR increases as the ribbon width decreases. The predicted edge modulus, which was predicted earlier, is considerably lower than a previous calculation using a different potential and the REBO potential is known to underestimate the bulk modulus. Initial Young modulus against the ribbon width for GNRs with unpassivated and hydrogen-passivated edges. The potential energy in Eq. (1) is modified account for the hydrogen adsorption, which has passivated edges.

H is the adsorption energy of Hydrigen per unit length along the edges of the GNR. The negative signs indicates typically reduced edge energy due to hydrogen passivation. While comparing the potential energies for the GNRs with or without H passivation, the adsorption energy can be determine as a function of the nominal strain for both armchair and zigzag edges. At the level of zero strain our MM calculations predict the hydrogen adsorption energy to be 20.5 and 22.6 eV/nm for the zigzag and armchair edges, respectively, which compare closely with the first principle calculations. The adsorption energy varies under uniaxial tension and it also varies with normal strain.

A negative edge modulus (20.5 0 = − e E eV/nm) is obtained in the latter case and thus the initial Young's modulus decreases with decreasing ribbon width, opposite to the unpassivated GNRs.

The horizontal dashed line in every single figure indicates the fracture strain of bulk graphene under uniaxial tension in the same direction. the bulk graphene fractures without any defect when the tangent modulus becomes zero (i.e., / 0 2 2 d U dε =), dictated by the intrinsic lattice instability under tension.

Fracture may occur much earlier due to thermally activated processes at a finite temperature. the critical strain to fracture for bulk graphene varies with the loading direction which was shown in an earlier study. first-principle calculations [22, 23] and empirical potential models both have predicted that the intrinsic critical strain is higher for graphene under uniaxial tension in the zigzag direction than in the armchair direction, suggesting that the hexagonal lattice of graphene preferably fractures along the zigzag directions by cleavage.

The GNRs with zigzag edges fracture at a critical strain close to that of bulk graphene loaded in the same direction as it is shown in Fig 1a. Fig. 1b shows a very contrastive way that the GNRs with armchair edges fracture at a critical (a) (b) strain considerably lower than bulk graphene. As shown in Fig 4, the fracture strain slightly depends on the ribbon width in both cases. The process of Hydrogen passivation of the edges leads to slightly lower fracture strains for zigzag GNRs, but slightly higher fracture strains for armchair GNRs. different fracture mechanisms for the zigzag and armchair GNRs are implied by the apparently different edge effects on the fracture strain. at different temperatures the processes of fracture nucleation in GNRs are studied by molecular dynamics (MD) simulations. Studies have proven that the edge effect leads to two distinct mechanisms for fracture nucleation in GNRs at relatively low temperatures (T < 300 K). Two fractured GNRs at 50 K are showen by the Fif 5. Fracture nucleation occurs stochastically at the interior lattice of the zigzag GNRs. For this very reason the fracture strain is very close to that of bulk graphene strained in the same direction, consistent with the MM calculations. For the GNR with armchair edges (Fig. 5b), fracture nucleation occurs most often near the edges. Leading to a lower fracture strain compared to bulk graphene, as seen also from the MM calculations, the armchair edge serves as the preferred location for fracture nucleation.

The same mechanisms hold for GNRs with H-passivated edges. Evidences of Fig 5 prove that that cracks preferably grow along the zigzag directions of the graphene lattice in both cases.

References

[1] Y. Ouyang, Y. Yoon, J. K. Fodor, and J. Guo, "Comparison of performance limits for carbon nanoribbon and carbon nanotube transistors", Applied Physics Letters, vol. 89, pp. 203107.1-203107.3, 2006.
[2] Pavel B. Sorokin, Pavel V. Avramov, Viktor A. Demin, Keonid A. Shernozatonskii, "Metallic Beta-Phase Silicon Nanowires:Structure and Electronic Properties",vol.1,13 Jun 2009.
[3] Jeroen W. G. Wilder, Liesbeth C. Venema, Andrew G. Rinzler, Richard E. Smalley & Cees Dekker, "Electronic structure of atomically resolved carbon nanotubes", Nature, Vol. 391, pp. 59, Jan 1998.
[4] Li, X., Cai, W., An, J. et al. 2009. Large-area synthesis of high-quality and uniform graphene films on copper foils. *Science* 324:1312–1314.
[5] Jeroen W. G. Wilder, Liesbeth C. Venema, Andrew G. Rinzler, Richard E. Smalley & Cees Dekker, "Electronic structure of atomically resolved carbon nanotubes", Nature, Vol. 391, pp. 59, Jan 1998.
[6] Mceuen, P.L. Lab. Of Atomic & Solid State Phys., Cornell Univ., Ithaca, NY Fuhrer, M.S. ; Hongkun Park, "Single-Walled Carbon Nanotube Electronics",Vol. 1,Issue: 1, pp. 78-85, Mar 2002
[7] G. Liang (NUS), Neophytos Neophytou (Purdue), Mark S. Lundstrom (Purdue), Dmitri Nikonov (Intel) , "Theoretical study of graphene nanoribbon field-effect transistors", 887.016 (Purdue University), Vol. 1,pp-127 – 130, Nanotech 2007
[8] Emtsev, K. V., Bostwick, A., Horn, K. et al. 2009. Towards wafer-size graphene layers by atmospheric pressure graphitization of silicon carbide. *Nat. Mater*. 8:203–207.
[9] Su, C.-Y., Lu, A.-Y., Wu, C.-Y. et al. 2011. Direct formation of wafer scale graphene thin layers on insulating substrates by chemical vapor deposition. *Nano Lett*. 11:3612–3616.
[10] Kholmanov, I. N., Magnuson, C. W., Aliev, A. E. et al. 2012. Improved electrical conductivity of graphene films integrated with metal nanowires. *Nano Lett.* 12:5679–5683.
[11] Yan, Z., Lin, J., Peng, Z. et al. 2012. Toward the synthesis of wafer-scale single-crystal graphene on copper foils. *ACS Nano* 6:9110–9117.
[12] Huang, P. Y., Ruiz-Vargas, C. S., van der Zande, A. M. et al. 2011. Grains and grain boundaries in single-layer graphene atomic patchwork quilts. *Nature* 469:389–392.
[13] Yamada, T., Kim, J., Ishihara, M. et al. 2013. Low-temperature graphene synthesis using microwave plasma CVD. *J. Phys. D: Appl. Phys.* 46:063001.
[14] Geng, D., Wu, B., Guo, Y. et al. 2012. Uniform hexagonal graphene flakes and films grown on liquid copper surface. *Proc. Natl. Acad. Sci. U.S.A.* 109:7992–7996.
[15] Vlassiouk, I., Smirnov, S., Regmi, M. et al. 2013. Graphene nucleation density on copper: Fundamental role of background pressure. *J. Phys. Chem. C* 117:18919–18926.
[16] Chen, S., Ji, H., Chou, H. et al. 2013. Millimeter-size single-crystal graphene by suppressing evaporative loss of Cu during low pressure chemical vapor deposition. *Adv. Mater.* 25:2062–2065.
[17] Wu, B., Geng, D., Guo, Y. et al. 2011. Equiangular hexagon-shape-controlled synthesis

of graphene on copper surface. *Adv. Mater.* 23:3522–3525.
[18] Jacobberger, R. M. and Arnold, M. S. 2013. Graphene growth dynamics on epitaxial copper thin films. *Chem. Mater.* 25:871–877.
[19] Sun, Z., Yan, Z., Yao, J. et al. 2010. Growth of graphene from solid carbon sources. *Nature* 468:549–552.
[20] Wu, W., Jauregui, L. A., Su, Z. et al. 2011. Growth of single crystal graphene arrays by locally controlling nucleation on polycrystalline Cu using chemical vapor deposition. *Adv. Mater.* 23:4898–4903.
[21] Ricardo Faccio, Pablo A Denis, Helena Pardo,Cecilia Goyenola ,and A lvaro WMombru, "Mechanical properties of graphene nanoribbons",J. Phys.: Condens.Matter, vol. 21, pp. 285304-285311, 2009
[22] Kwon, S.-Y., Ciobanu, C. V., Petrova, V. et al. 2009. Growth of semiconducting graphene on palladium. *Nano Lett.* 9:3985–3990.
[23] Ramón, M. E., Gupta, A., Corbet, C. et al. 2011. CMOS-compatible synthesis of largearea, high-mobility graphene by chemical vapor deposition of acetylene on cobalt thin films. *ACS Nano* 5:7198–7204.

Chapter 3

Electromagnetic properties of Graphene Nano-Ribon

3.1 Basic Electronic Properties of Graphene Based Structures

As illustrated in Figure 1.1a, Graphene is defined as a single layer of carbon atoms arranged in a hexagonal lattice. To construct other carbon based materials ots atomic structure can also be used as a basic building block. It can be used in several ways like folded into fullernes, rolled up into nanotubes or stacked into graphite. The primitive cell of grapheme is made of two non-equivalent atoms. They can be identified as A and B and these two sublattices are translated from each other by a carbon-carbon distance **a=1.44.**

A singular Carbon atom contains four valence electrons with a ground state electronic shell configuration of [He] $2s^2$ $2p^2$.The carbon-carbon bond in grapheme are hybridized orbitals generated by the superposition of 2s with $2p_x$ and $2p_y$ orbitals. The energetically stable and localized sigma bonds are formed by the planar orbitals with the three nearest neighbor carbon atoms in the honeycomb lattice. They are actually responsible for the most of the blinding energy and for the elastic properties of the grapheme sheet [1]. The remaining free $2p_z$ orbitals present 'pi' symmetry orientation. The overlapping of these orbital states between neighbouring atoms plays a major role in the electronic properties of grapheme. That is why, a good approximation for describing the electronic structure of grapheme is to adopt orthogonal nearest neighbor tight binding approximation assuming that its electronic states can be simply represented by a linear combination of $2p_z$ orbitals. One can obtain the energy dispersion relation of pi bonding and pi antibonding bands through solving the equation of Schrodinger Equation.

Here k_x and k_y are the components of the k vector that are folded onto the first hexagonal Brillouin zone and gama= 2.75 eV is the desired energy[2]. Closed form expressions which obtained analytically for the single electron propagators written on a real space basis. One can see in Figure 1.1b that the band structure of grapheme is obtained from such a simple tight binding model. This yields symmetric conduction and valence bands with respect to the Fermi energy set at 0 e.V. Located on the corners of the Brillouin zone, the grapheme valence and conduction bands degenerate at 6 points[3].

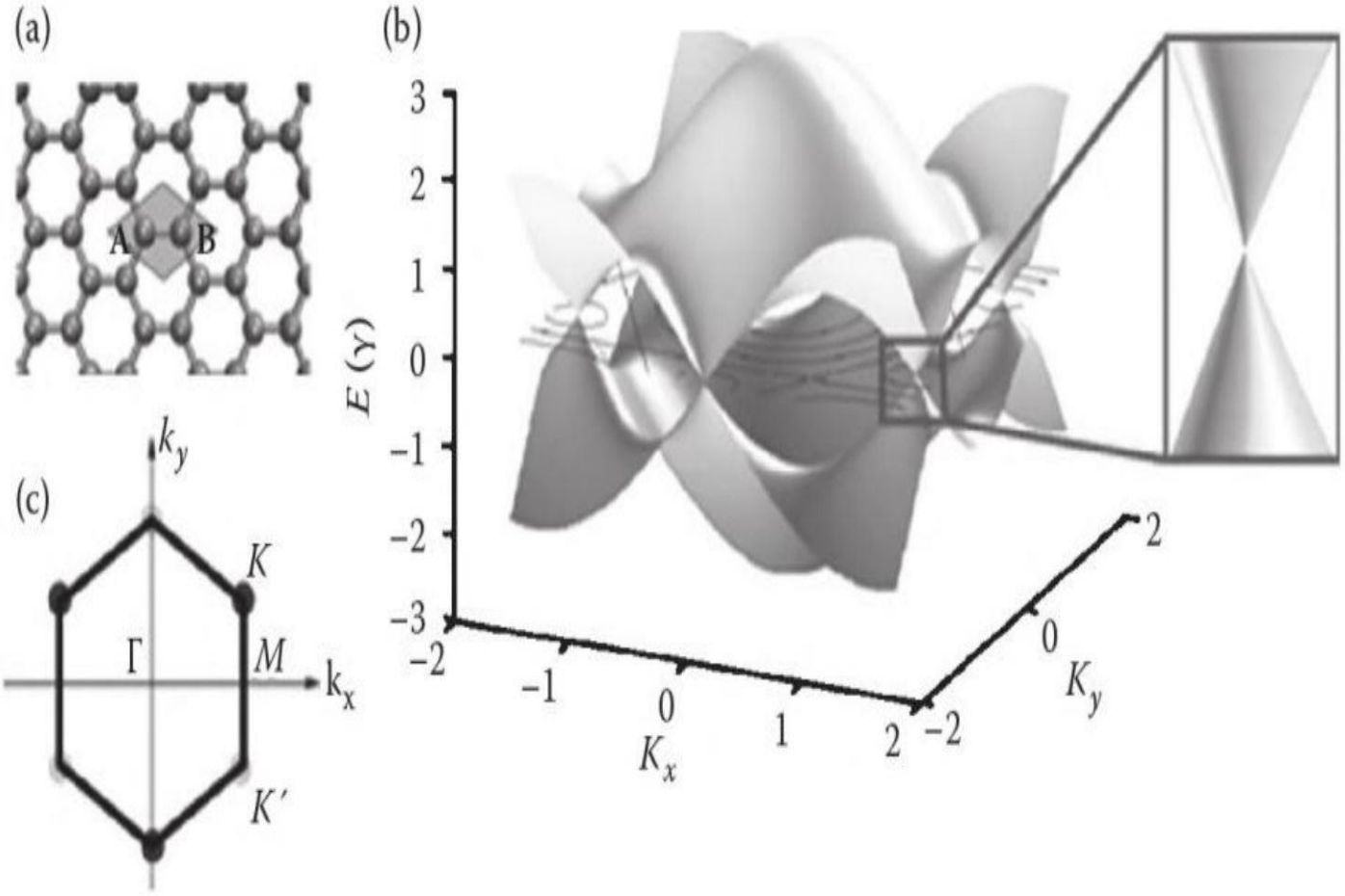

Figure(3.1) (a) Honeycomb lattice of Graphene. (b) Bang energy dispersion obtained via tight binding approximation. (c) First Brillouin Zone.

3.2 Band Gap engineering of Graphene Nano-Ribbon

The graphene band structure already proved that this material is a zero-gap semiconductor. Many electronics applications rely on the use of a semiconductor with a finite band gap and this energy barrier to charge transport can be used to control electron flow. This fact brings us to the central theme of this dissertation. It is already showed that by curving grapheme into a narrow ribbon or a Graphene nanoribbon it is possible to induce a transport gap in the grapheme spectrum. We can understand the induced transport gap in graphene nanoribbons in terms of an energy gap arising from simple quantum confinement from a heuristic approach. The band gap depends on the diameter and chirality of the tube for carbon nanotubes. It has been proved the band gap of a graphene nanoribbon will depend on its width and crystallographic orientation.

First estimate of the width and the size dependence of the band gap in a graphene nanoribbon, they carried out a "back-of-the-envelope" calculation for the allowed energies expected in a graphene nanoribbon. The two ingredients to their calculation are

(i) Quantum confinement in one dimension, and
(ii) Graphene's linear dispersion at low energies.

Quantum confinement in the x-direction results in allowed wavefunctions:

$$\psi(x) \propto \sin(k_x x) \text{ with } k_x = n\pi/W \text{----------(3.1)}$$

Where *n* is an integer. We then introduce the dispersion relation

$$E \approx \hbar v_F (K_x^2 + K_y^2)^{1/2} \text{----------(3.2)}$$

For obtaining allowed energy levels

$$En = (n\hbar v_F \pi)/W \text{---------- (3.3)}$$

so that the gap between levels is

$$E_{gap} = (\hbar v_F \pi)/W \text{ ---------- (3.4)}$$

Here, W is the width of the GNR

Ħ is the plunk constant

vF is the Fermi velocity considered as $8*10^8$

π is considered as 3.1416

With the value of each parameter I have drown a figure(3.2) where the relation between width and Band Gap are showed .

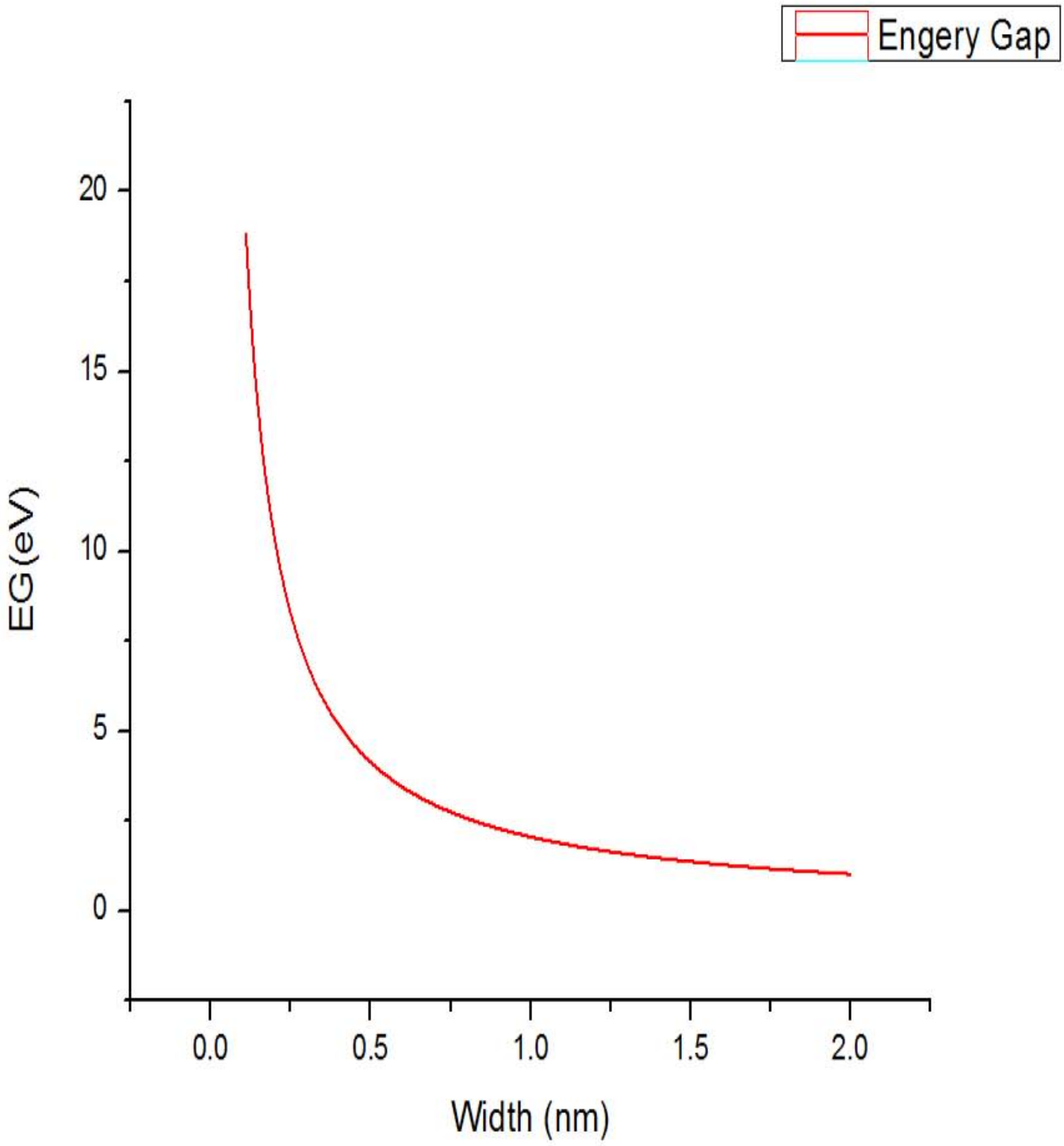

Figure(3.2) : Changing of Energy Band Gap with respect to width.

Here, from the figure (3.2) we have seen that with respect to width the energy band Gap is decreasing respectively.

3.3 Electromagnetic Properties for GNR interconnect

To see the effect of conductance for Graphene Nano-Ribbon, we took a RLC circuit model with GNR interconnect. We got some equation from there. Which help us to saw the conductance effect of GNR.

There are two terminals named as P and N. P represent positive and N represent Negative terminal of a GNR interconnect. This circuit is a distributed RLC equivalent circuit for GNRs which considered in the model. In this model there are few parameter:

R_Q represent the quantum contract resistance.

R represent the GNR resistance per unit length.

I_M Represent magnetic inductance per unit length of GNR.

I_K represent the kinetic inductance per unit length of GNR.

C_Q and **C_E** are the GNR quantum capacitance and electrostatic capacitance per unit length. Also it is noticeable that terminal **P** and **N** are symmetric, completely interchangeable.

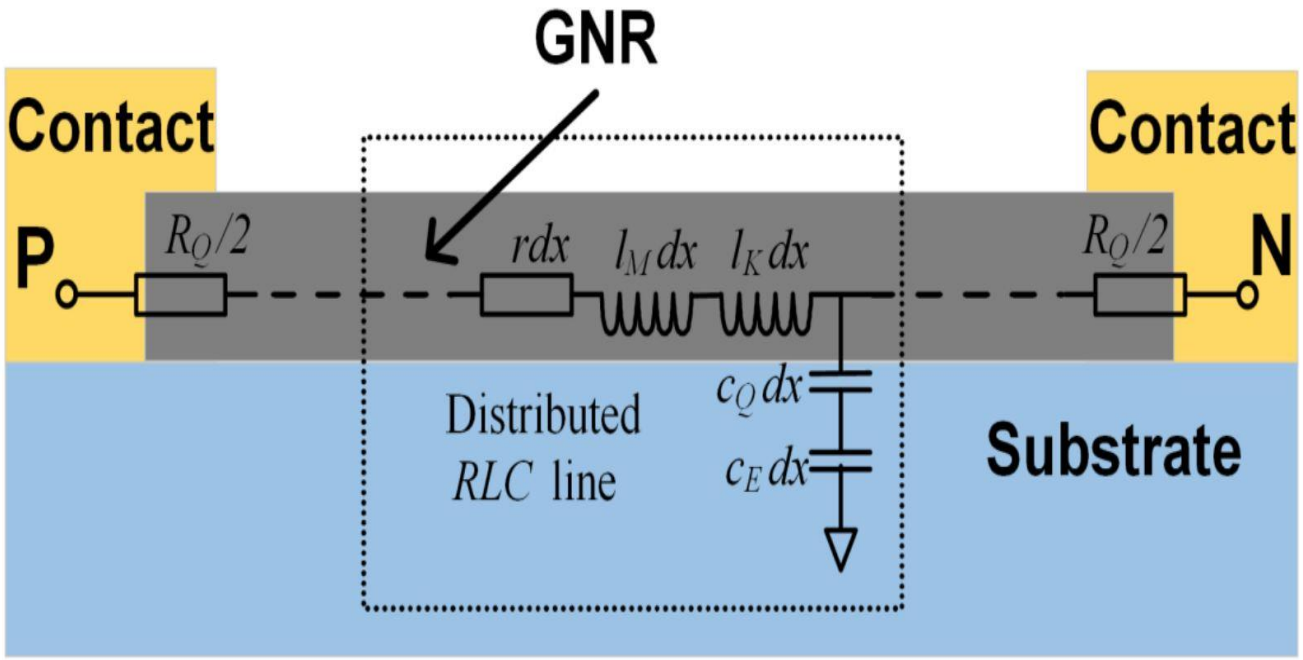

Figure(3.3): Schematic of a GNR interconnect and corresponding RLC distributed circuit model

3.3.1 GNR Resistance

Depending on the linear response Laudauer formula, single GNR layer *Gn* can be expressed for the conductance of the nth conduction mode as

$$G_n = 2q^2/h. \int T_n(E) (-\partial f_0/\partial E)\, dE \quad \text{---------- (3.1)}$$

$$f_0(E) = \{1+ \exp[(E-E_F)/K_BT]\}^{-1} \quad \text{---------- (3.2)}$$

Here,

Tn(*E*) represents the transmission coefficient,

f0(*E*) represents the Fermi-Dirac distribution function.

EF is the Fermi level.

kB is the Boltzmann's constant.

T represent the temperature.

Using the Matthiessen's rule, *Tn*(*E*) can be obtained by

$$\frac{1}{T_n(\mathrm{E})} = 1 + \frac{L}{l_D \cos\theta} + \frac{L}{w \cot\theta} \approx \frac{L}{l_D \cos\theta} + \frac{L}{w \cot\theta} \quad \text{----------(3.3)}$$

Here, **lD** is the carrier mean free path.

w is the width of GNR.

cot*θ* represent the ratio of longitudinal to transverse velocities. In (3.3).

The term "1" is due to quantum conductance, which can be ignored when *L* >> *lD*.

A single GNR layer's total conductance is the summation of conductance of electrons and holes, as in (3.3).

$$G_{total} = \sum_n G_n(\text{electrons}) + \sum_n G_n(\text{holes}) \quad \text{----------(3.4)}$$

Transforming it to integration form, we can write

$$G_{total} = \frac{2}{\Delta E_n}\left[\int_0^{\infty} G_n(\text{electrons})\,\mathrm{d}E_n + \int_{-\infty}^{0} G_n(\text{holes})\,\mathrm{d}E_n\right]$$

--------(3.5)

We can derive it as

$$G_{total} = \frac{4q^2w^2}{Lh^2v_f}\cdot 2k_BT\ln\left[2\cosh\left(\frac{E_F}{2k_BT}\right)\right]\cdot func(w,l_D)$$

----------*(3.6)*

func(*w*, *lD*) is defined as

$$func(w,l_D) = \begin{cases} \dfrac{\pi w - 2l_D}{l_D} + \dfrac{4\sqrt{l_D^2 - w^2}}{l_D}\cdot \operatorname{arctanh}\left(\sqrt{\dfrac{l_D - w}{l_D + w}}\right), & l_D \geq w \\ \dfrac{\pi w - 2l_D}{l_D} - \dfrac{4\sqrt{l_D^2 - w^2}}{l_D}\cdot \arctan\left(\sqrt{\dfrac{l_D - w}{l_D + w}}\right), & l_D < w \end{cases}$$

----------(3.7)

With the proper value of parameters, we can see effect of change of resistance with respect to width.

Considering,

W= 10nm to 100nm.

Id= 1*10^-6;

H= plank's constant

Vf=8*10^6;

L=100*10^-9;

q= 1.602*10^-19;

T=300;

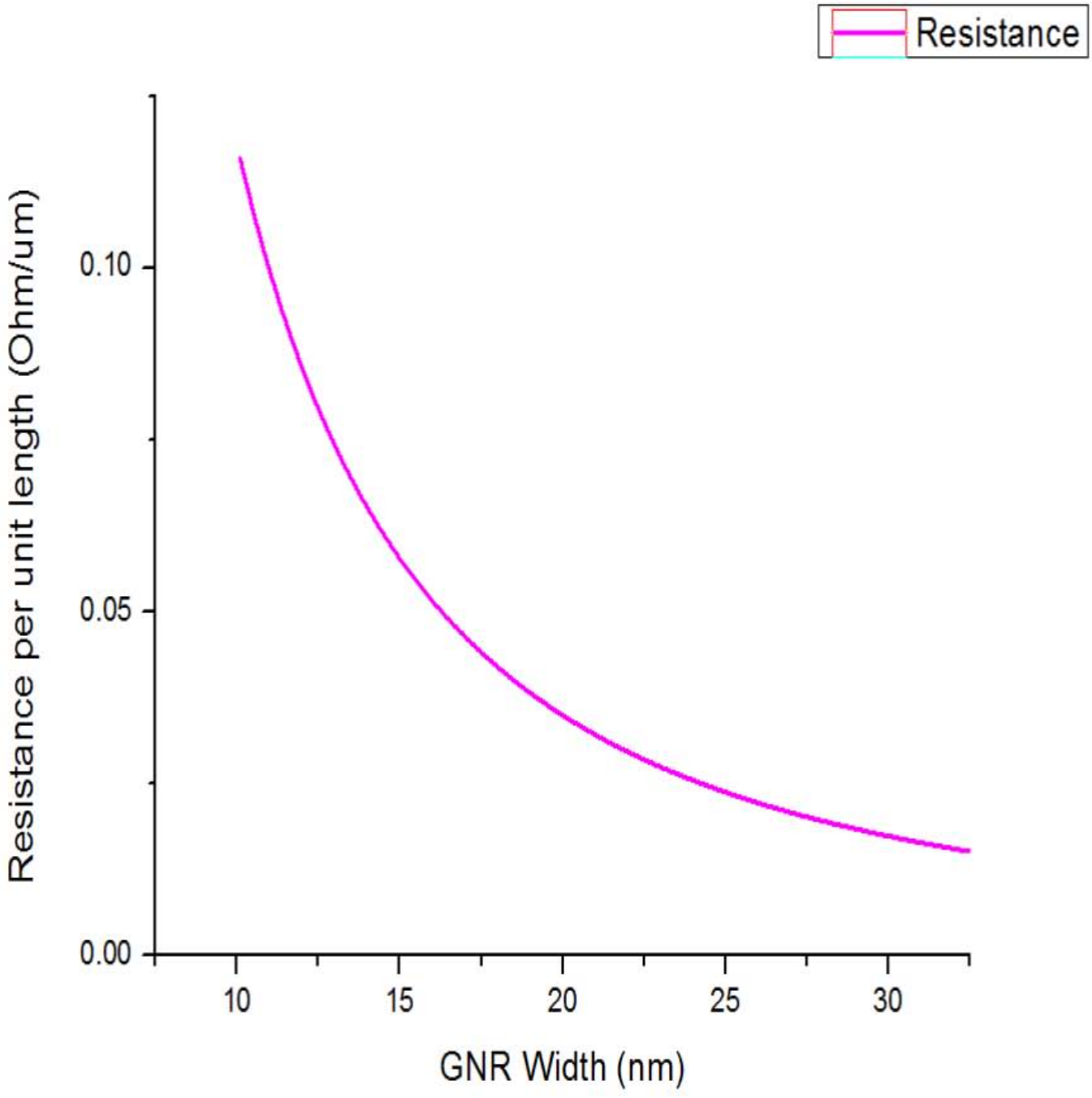

Figure(3.4) : changes of Resistance with respect to Width.

Equation of the Resistance with respect to Number of layer and number of channel of Graphene Nano-Ribbon. The quantum contact resistance of GNR is defined as :

$R_Q = (h/2q2) / N_{ch} N_{layer}$ ---------- (3.8)

Here, h= plank's constant;

q= charge of electrons;

Nch= number of conducting channel mode of GNR;

Nlayer= number of layer of GNR.

3.3.2 Capacitance

The capacitance per unit length is calculated by neglecting the electrostatic capacitance in the current version of GNR interconnect model:

$C_{total} = C_Q = (N_{layer} N_{ch} 4q^2)/ hv_f$; ----------(3.9)

Here,
v_f represent the Fermi velocity.

3.3.3 Inductance

The inductance per unit length by neglecting the magnetic inductance in the current version of GNR interconnect model is calculated as

$L_{total} = l_K = (h/4q2\ vf)/ N_{layer} N_{ch}$; ----------(3.10)

Number of conducting channel mode (N_{ch}) can be calculated by using below theorem:

$$N_{ch} = N_{ch,electron} + N_{ch,hole} = \sum_n \left[1+\exp\left(\frac{E_{n,electron} - E_F}{k_B T}\right)\right]^{-1} + \sum_n \left[1+\exp(\frac{E_F - E_{n,hole}}{k_B T})\right]^{-1}$$

----------(3.11)

Here,

Where, *En, electron* (*En, hole)* is the minimum energy of the *n*th conduction sub band.

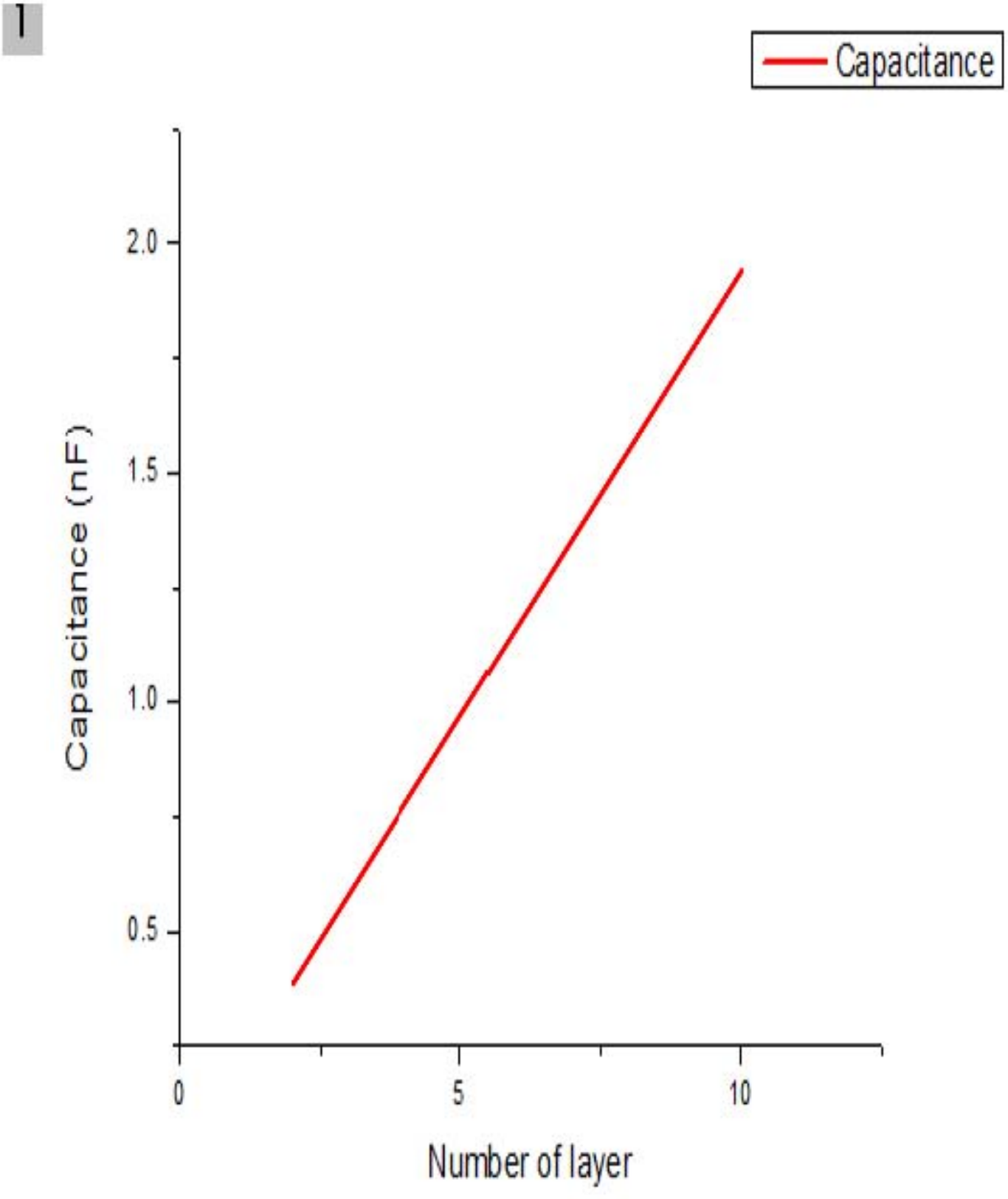

Figure(3.5): Change of capacitance with respect to Number of layer

1

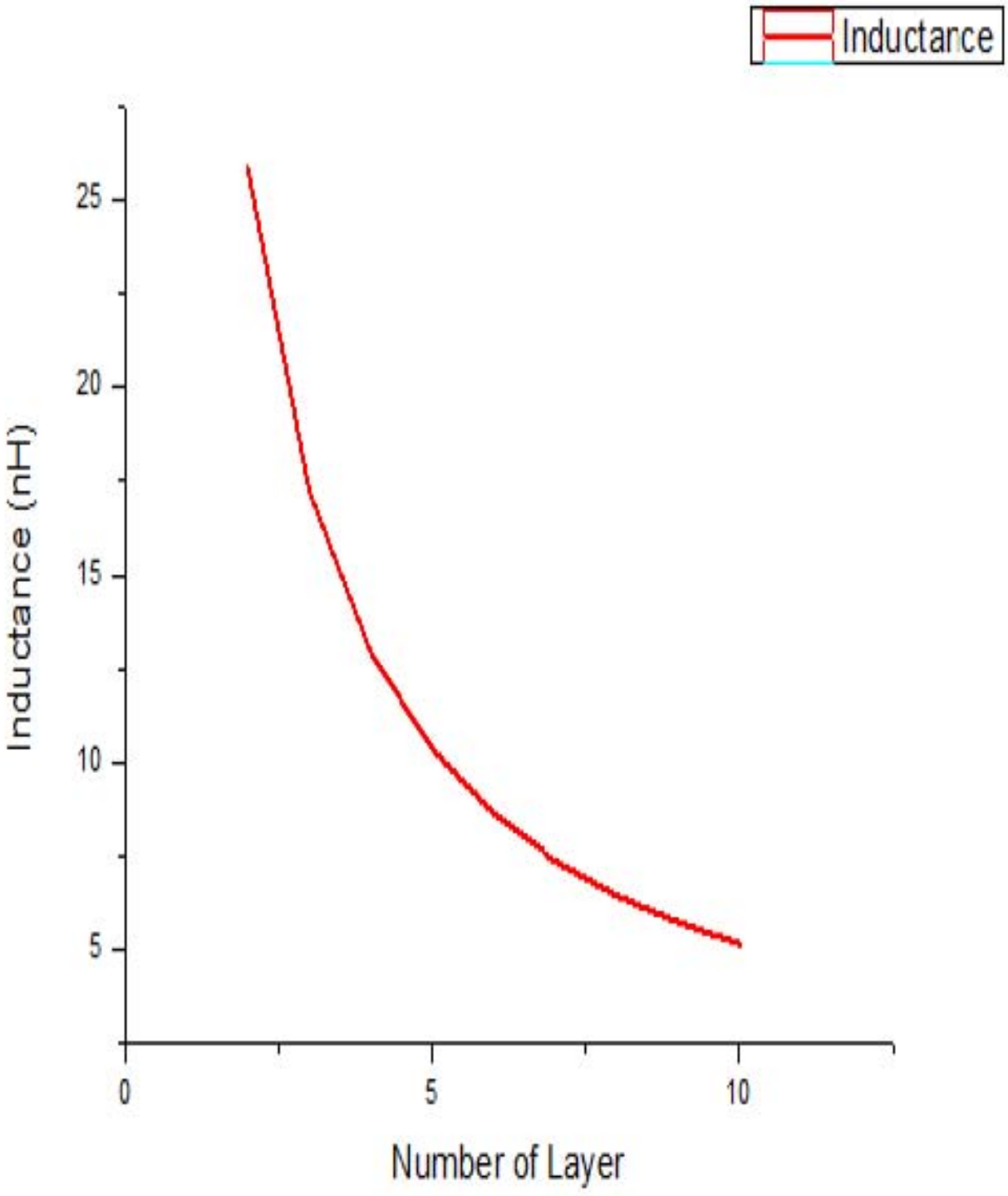

Figure(3.6): Changes of inductance with respect to number of layer

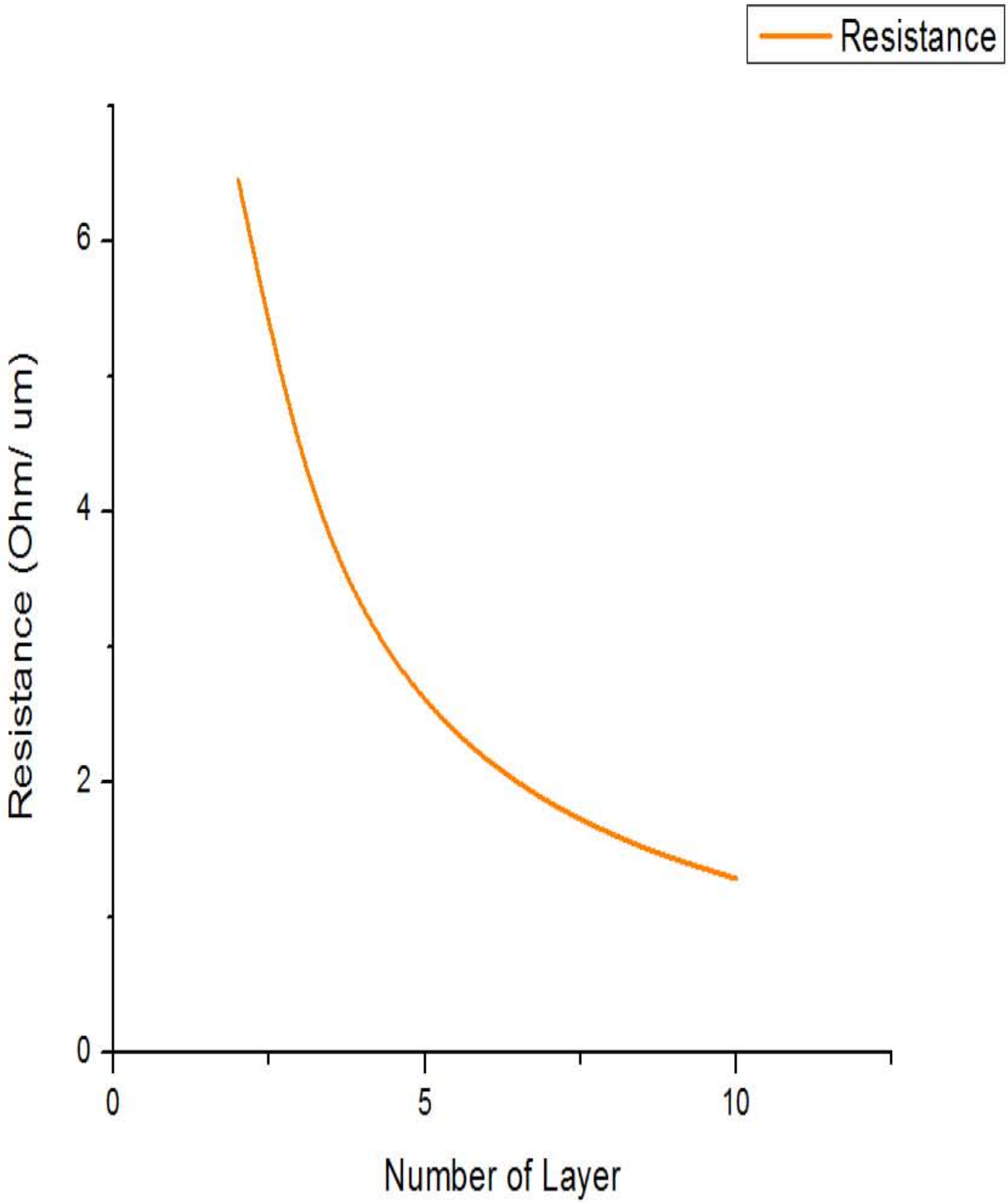

Figure: Resistance of Graphene Nano-Ribbon with respect to number of layer

Reference

[1] [26] K. Tanaka, S. Yamashita, H. Yamabe, and T. Yamabe, Synthetic Metals **17**, 143 (1987).
[2] S. E. Stein and R. L. Brown, Journal of the American Chemical Society **109**, 3721 (1987).

[3] L. Jiao, L. Zhang, X. Wang, G. Diankov, and H. Dai, Nature **458**, 877 (2009).

[4] M. Y. Han, J. C. Brant, and P. Kim, Physical Review Letters **104**, 056801 (2010).

[5] M.C.Lemme, t. j. Echtermeyer M.Baus and H.Kurz, 'A grapheme field effect device'. IEEE electron Device let. Vol. 28. No. 4, pp. 282-284, Apr. 2007

[6] C. X, hH. Matsubara, and S. Murakami ,' properties pf AsF5 intercalateds vapor-grown graphite,'Synth. M<et., vol. 14 no. ½,pp. 113-123. Mar 1086

[7] A. Nieuwoudt and Y. Massoud. Understanding the impact of inductance in carbon nanotube bundles for VLSI interconnect using scalable modeling techniques, *IEEE Transactions on Nanotechnology*, 5(6), 758–765, 2006.
[8] N. Srivastava, H. Li, F. Kreupl, and K. Banerjee. On the applicability of single-walled carbon nanotubes as VLSI interconnects. *IEEE Transactions on Nanotechnology*, 8(4), 542–559, 2009.
[9] A. Naeemi and J. D. Meindl. Compact physics-based circuit models for graphene nanoribbon interconnects, *IEEE Transactions on Electron Devices*, 56(9), 1822–1833, 2009.

Chapter 04

Application of Graphene Nano-Ribbon (GNR)

4.1 Application of Graphene and Graphene Nano-Ribbon

There are lots of application of Grpahene and GNR. Few of them are described below:

4.1.1 Photonic

A photodetector is the key component to optoelectronic devices and it is one of the potential photonic applications of graphene. With traditional semiconductors in contrast, pristine graphene has no bandgap, which means that is has broader wavelength absorption for broadband photodetection. Meanwhile, ultrahigh carrier mobility makes graphene suitable for ultrafast photodetection. It has been shown by high-frequency measurement that there is no performance degradation in graphenebased photodetectors up to 40 Hz, and the intrinsic bandwidth of graphene can be as high as 500 Hz, comparable with the fastest III–V semiconductor-based ones [1]. However, graphene-based photodetectors usually have low photocurrent responsibility because of the low optical absorption of single-layer graphene. Coupling with plasmonic structures is one effective way to enhance the photocurrent. It has been reported that the photocurrent of gold-decorated graphene was more than one order of magnitude higher than that of pristine graphene [2].

Another potential application of graphene is an optical modulator. Due to its high speed and broad bandwidth, it can be widely used in on-chip optical interconnects to substitute currently used electric interconnects. Compared with traditional semiconductors, graphene shows advantages in high carrier mobility, large optical bandwidth, and strong modulation ability, which makes graphene suitable for highperformance optical modulators. A graphene-based optical modulator has recently been demonstrated [3]. It has an operation frequency as high as 1 GHz. Moreover, its optical bandwidth can range from 1.35 to 1.6 μm, while its footprint is only 25 μm2, which was much better than the current modulators.

Polarizers Graphene can convert undefined lights to polarized lights. The polarizing properties can be simply tuned by changing the Fermi level of graphene. In addition, graphene polarizers can cover a much wider bandwidth than current polarizer materials. By integrating graphene within an optical fiber, the device exhibits a strong s-polarization extinction ratio of 27 dB, which is comparable to current metal-based polarizers, but the graphene-based polarizer can work in a much broader wavelength range—from 800 to 1650 nm—indicating the appealing potential of graphene in the application of high-performance polarizers [4].

4.1.2 Thermal management

In current electronic and photonic technologies, low operation temperature and efficient heat dissipation are important for life and operation speed of devices. Graphene is proposed as a material for heat removal due to its extraordinarily high intrinsic thermal conductivity. The room temperature thermal conductivity of suspended graphene was determined to range from 3080–5300 W m–1 K–1. Moreover, graphene has very high electron mobility and low resistivity. The unique thermal and electrical properties of graphene make it a potentially promising material for thermal management [5,6].

Monolayer graphene synthesized by CVD can be used for the application of heat spreader in electronic packing. The hot-spot temperature is decreased by ~5°C at a heat flux of up to 800 W cm–2. This result can be further improved by optimizing the synthesis parameters and transfer process. In silicon-on-insulator (SOI) metal-oxide-semiconductor field-effect transistor (MOSFET) structure, the buried oxide insulates the active channel from the substrate both electrically and thermally, which results in temperature rise and leads to performance degradation and early thermal breakdown. In order to resolve this problem, graphene can be adopted as the material for lateral heat spreaders, which can lead to great reduction in temperature of the hot spots.

Graphene is also a novel promising candidate for gap-filling thermal interfacial material in electronic and photonic devices. Graphene stacked in a 3-D structure in the electrodes of an electrical device is beneficial for rapid ion dissipation and making full use of a specific surface area. A 3-D vertically aligned graphene architecture between a silicon surface and an exploration has great potential in thermal management of electronic and photonic applications.

4.1.3 Electronics

A promising potential for the fast operating speed of graphene-based transistors is given by the ultra-high intrinsic carrier mobility of Graphene. In addition, the peak intrinsic average carrier velocity of graphene was theoretically calculated to be four times higher than Si. Therefore, graphene is suitable to be used in high-frequency devices, which is of great importance in the application of communication technologies such as wireless transmission and signal processing. The research group from IBM demonstrated the first experimental study on high-frequency top-gated devices made of graphene transistors. A high cutoff frequency of 26 GHz was obtained with a channel length of 150 nm [7]. Later, the IBM research group further demonstrated that the cutoff frequency could be increased to 100 GHz with a gate length of 240 nm when using graphene epitaxially grown on SiC [8]. Recent research has moved the frequency forward to 280 GHz in 40-nm length channels. Chemical vapor deposition grown graphene has also been fabricated into high-frequency devices. Graphenebased radio-frequency transistors with a gate length of 40 nm could reach a cutoff frequency of 155 GHz [9]. Although exceptionally high switching speed has been realized in graphene-based transistors, the lack of inherent bandgap limits the application of graphene in logic circuits. As a result, there have been numerous efforts to generate and tune the bandgap in graphene to meet different application demands. Methods such as fabrication of nanostructures of graphene using bilayer or trilayer graphene or generating strains in graphene have been developed, and successful formation and control of the bandgap has been achieved, which is of practical importance for graphene in various devices.

4.1.4 Energy conversation and storage

Graphene is currently being widely studied in the application of the lithiumion (Li-ion) battery [10], which is a renewable and clean power source for portable devices, electrical/hybrid vehicles, and miscellaneous power devices. As many potential electrode materials (graphite or transition metal oxide) in a Li-ion battery suffer from slow Li-ion diffusion, poor electron transport, and increased resistanceat high charge-discharge rates, graphene-based electrode materials in Li-ion batteries have been proposed as one of the promising alternatives due to graphene's high electrical conductivity and typical 2-D structure [11,12]. Graphene itself can be used as a high-capacity anode material [49]. More importantly, graphene acting as a conducting agent with unique 2-D nanostructure is helpful for fabrication of novel structures with various active materials and enormously improving their electrochemical performance. So far, numerous graphene-based composite cathode and anode materials have been successfully prepared, and their outstanding charge/ discharge performance show the broad future of graphene in the application in Li-ion batteries [13,14].

4.1.5 Sensors

Many graphene-based electrochemical sensors have been reported to detect dopamine, glucose, hydrogen peroxide (H2O2), ascorbic acid, antigen, and deoxyribonucleic acid (DNA). Graphene-based materials can not only be developed for environmental electrochemical analysis of some toxic and explosive substances, but can also be used as enhancing material for toxic arsenic removal. In addition, the gas-sensor properties of graphene have been investigated by many groups [58]. Graphene-based gas sensors can be widely used to detect various gases such as nitrogen dioxide (NO2), ammonia (NH3), and carbon monoxide (CO). These different kinds of sensors fabricated by graphene have two advantages. One advantage is their multifunctionality—a single device can be utilized in various measurements (e.g., pressure, gas environment, and magnetic field), which offers unique opportunities. The other advantage is that its extremely high sensitivity makes any measurement more precise, which is especially important within the fields of advanced technology. With the development of increasingly interactive consumer electronic devices and the advancement of the technology, such graphene sensors will certainly find their way into a large body of products in the near future.

4.1.6 Bio applications

The growing demand for the analysis of genomes of many species and cancers, along with the ultimate goal of deciphering individual human genomes, has led to the development of non-Sanger reaction-based technologies toward rapid and inexpensive DNA sequencing. Graphene was considered to be a great potential material for resolving this problem. It is envisioned that porous graphene can be prepared via a certain method and the size of nanopores matched well with the width of DNA, allowing a DNA molecule through the pores. The influences of the four DNA bases (A, C, G, T) on the conductivity of graphene are different, therefore it is easy to determine which

base is passing through the pores by measuring the voltage deference during the passage [15]. Some scientists even find that sheets of GO are highly effective at killing bacteria.

4.1.7 Potential Application of GNR

In Graphene Nano-Ribbon both H-terminated GNRs and alkylated GNRs have a broad range of potential applications. The most apparent is the incorporation of GNRs in polymer hosts for the fabrication of novel composite materials. GNRs have the same high aspect ratio as their parent MWCNTs, but differences in their nanostructure produce unique and unexpected results. For example, the incorporation of GNRs into a dielectric polymer host dramatically changes its electric properties12,13 in a way that is significantly different from that achieved by incorporation of MWCNTs. The most intriguing result is that GNR containing polymer composites possess remarkably low loss (<0.02) at reasonably high permittivity values (Figure 4.1). This is important because the miniaturization of electronic components requires materials with high permittivity and low loss in the radio and low microwave frequency region. In the high frequency microwave region, low loss is critical for antennas and other military applications. By varying the type and content of GNRs, the loss and permittivity of composites can be tuned to desirable values over a wide range. The dielectric constant can be tuned from moderate to extremely high (>1,000) values, while the corresponding loss tangent can be varied from ultralow (<0.02) to high (~1.0) . [16]

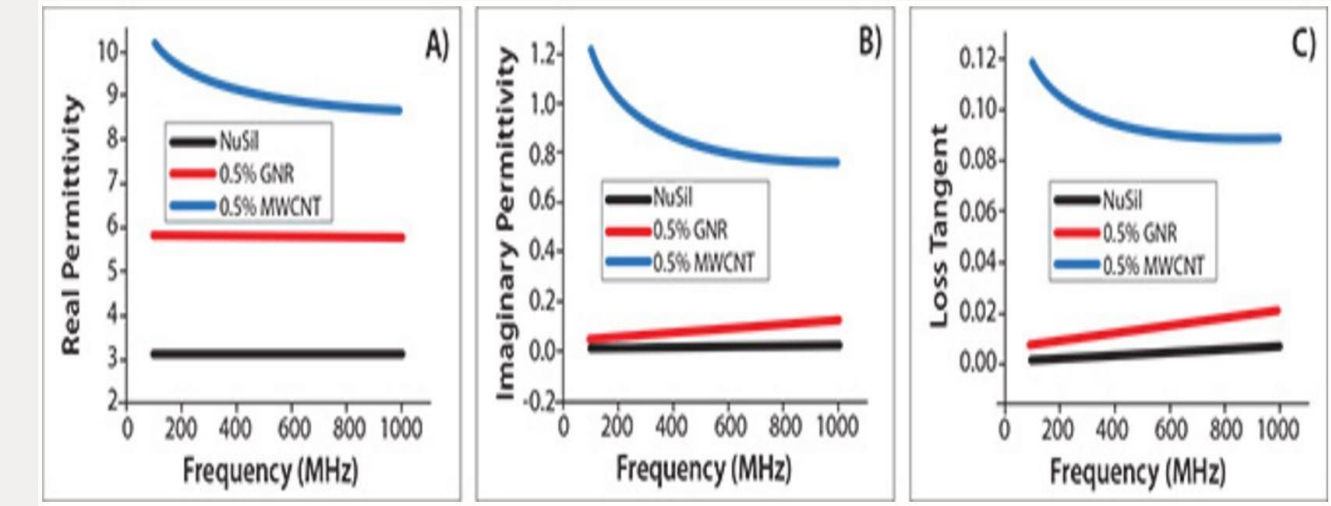

Figure(4.1): Dielectric properties of the GNR/NuSil (silicon elastomer) composites. (A) Real permittivity, (B) imaginary permittivity, and (C) loss tangent of pure NuSil (black), MWCNT/NuSil (blue), and GNR/NuSil (red) composites containing 0.5 wt % incorporated conductive filler.

References

[1] Liu, X.-W., Mao, J.-J., Liu, P.-D. and Wei, X.-W. 2011. Fabrication of metal-graphene hybrid materials by electroless deposition. *Carbon* 49(2):477–483.

[2] Liu, S., Wang, J., Zeng, J. et al. 2010. "Green" electrochemical synthesis of Pt/ graphene sheet nanocomposite film and its electrocatalytic property. *J. Power Sources* 195(15):4628–4633.

[3] Hu, Y., Zhang, H., Wu, P., Zhang, H., Zhou, B. and Cai, C. 2011. Bimetallic Pt–Au nanocatalysts electrochemically deposited on graphene and their electrocatalytic characteristics towards oxygen reduction and methanol oxidation. *Phys. Chem. Chem. Phys.* 13(9):4083–4094.

[4] Zhang, H., Xu, X., Gu, P., Li, C., Wu, P. and Cai, C. 2011. Microwave-assisted synthesis of graphene-supported Pd1Pt3 nanostructures and their electrocatalytic activity for methanol oxidation. *Electrochim. Acta* 56(20):7064–7070.

[5] Yun, Y. S., Kim, D., Tak, Y. and Jin, H.-J. 2011. Porous graphene/carbon nanotube composite cathode for proton exchange membrane fuel cell. *Synth. Met.* 161(21):2460–2465.

[6] Rajesh, Paul, R. K. and Mulchandani, A. 2013. Platinum nanoflowers decorated threedimensional graphene–carbon nanotubes hybrid with enhanced electrocatalytic activity. *J. Power Sources* 223:23–29.

[7] Seger, B. and Kamat, P. V. 2009. Electrocatalytically active graphene-platinum nanocomposites. Role of 2-D carbon support in PEM fuel cells.*J. Phys. Chem. C*113(19):7990–7995.

[8] Yoo, E., Okata, T., Akita, T., Kohyama, M., Nakamura, J. and Honma, I. 2009. Enhanced electrocatalytic activity of Pt subnanoclusters on graphene nanosheet surface. *Nano Lett.* 9(6):2255–2259.

[9] Zhou, Y.-G., Chen, J.-J., Wang, F.-B., Sheng, Z.-H. and Xia, X.-H. 2010. A facile approach to the synthesis of highly electroactive Pt nanoparticles on graphene as an anode catalyst for direct methanol fuel cells. *Chem. Commun.* 46(32):5951–5953.

[10] Huang, Z., Zhou, H., Li, C., Zeng, F., Fu, C. and Kuang, Y. 2012. Preparation of welldispersed PdAu bimetallic nanoparticles on reduced graphene oxide sheets with excellent electrochemical activity for ethanol oxidation in alkaline media. *J. Mater. Chem.* 22(5):1781–1785.

[11]. Liu, J., Zhou, H., Wang, Q., Zeng, F. and Kuang, Y. 2012. Reduced graphene oxide supported palladium–silver bimetallic nanoparticles for ethanol electro-oxidation in alkaline media. *J. Mater. Sci.* 47(5):2188–2194.

[12] Lee, S. H., Kakati, N., Jee, S. H., Maiti, J. and Yoon, Y.-S. 2011. Hydrothermal synthesis of PtRu nanoparticles supported on graphene sheets for methanol oxidation in direct methanol fuel cell. *Mater. Lett.* 65(21):3281–3284.

[13] Yang, G., Li, Y., Rana, R. K. and Zhu, J.-J. 2013. Pt–Au/nitrogen-doped graphene nanocomposites for enhanced electrochemical activities. *J. Mater. Chem. A* 1(5):1754–1762.
[14] . Hu, Y., Wu, P., Zhang, H. and Cai, C. 2012. Synthesis of graphene-supported hollow Pt–Ni nanocatalysts for highly active electrocatalysis toward the methanol oxidation reaction. *Electrochim. Acta* 85:314–321.

[15] Vinayan, B. P., Nagar, R., Rajalakshmi, N. and Ramaprabhu, S. 2012. Novel platinumcobalt alloy nanoparticles dispersed on nitrogen-doped graphene as a cathode electrocatalyst for PEMFC applications. *Adv. Funct. Mater.* 22(16):3519–3526.

[16] Dimiev, A. M.; Zakhidov, D.; Genorio, B.; Oladimeji, K.; Crowgey, B.; Rothwell, E. J.; Kempel, L. C.; Tour, J. M. Permittivity of dielectric composite materials comprising graphene nanoribbons, The effect of nanostructure. ACS Appl. Mater. Interfaces 2013, 5, 7567–7573. - See more at: http://www.sigmaaldrich.com/technical-documents/articles/materials-science/graphene-nanoribbons-production-and-applications.html#ref

Chapter 5

Conclusion And Future work

5.1 Conclusion

With whole work of mine, I have analyzed the properties of Graphene Nano-Ribbon. I have considered a circuit diagram to see the effect of the number channel to electromagnetic properties of Graphene Nano-Ribbon. I have showed that how resistance related to the width of the grapheme nano-ribbon. I have tried to find out how many channel we should consider to get the best performance from Graphene Nano-Ribbon. I have showed all three elements a single graph to get a better view to decide how many layer we should use. I have also showed the relation between width and energy band Gap of GNR. With increasing of number of channel, the resistance and the inductance get low but on the other hand the capacitance get increased. So we eagerly needed a specific number of channel which will be the best to consider for the GNR. In my entire thesis, I have done all of this work.

5.2 Future work

In my above thesis I have worked with the number of channel of GNR and some effect of width with electromagnetic properties of GNR. But in future work, I would prefer to see all of this effect in response of frequency. And also I want to compare the performance of GNR with Carbon Nano-tube (CNT) and also with cooper for a specific model of antenna.

Chapter 6

Appendix

1. MATLAB code for Energy Band Gap of grapheme nano-Ribbon with respect to Width.

```
h=1.054571800*10^-34;
 Vf=10^6;
 w=0.1e-9:0.01e-9:2e-9;
Egap=(h*Vf*pi)./w;
 plot(w,Egap)
xlabel('width')
ylabel('Egap')
fid = fopen('EGAP.doc','w');
fprintf(fid,'%10.20f\n',Egap);
fclose(fid);
fid = fopen('width.doc','w');
fprintf(fid,'%10.10f\n',w);
fclose(fid);
```

2. MATLAB code for Resistance with respect to width.

```
q=1.602e-19;
 w=10e-9:0.1e-9:45e-9;
 Id=1e-6;
 h=6.626e-34;
 Vf=8e5;
L=1e-6; Q=(1/L)*((2*(q^2))/h).*((2.*(w.^2))./(h*Vf));
Kb=1.38e-23;
 T=300;
 Ef=-0.21*(1.6e-19);
Part=(2*Kb*T.*((log(2*cosh(Ef/(2*Kb*T))))/(log(exp(1)))));
 Func=(2.*(log(Id./w)./(log(exp(1))))+(2*log(2)/(log(exp(1))))-2+((pi.*w)./Id));
Z=Q.*Func.*Part;
Y=1./Z;
plot(w,Y);
xlabel('Width(nm)');
ylabel('Resistance');
w=w.*1e9;
Y=Y.*1e-6;

fid = fopen('widthr.doc','w');
```

```
fprintf(fid,'%10.10f\n',w);
fclose(fid);
fid = fopen('resistance.doc','w');
fprintf(fid,'%10.10f\n',Y);
fclose(fid);
```

3. MATLAB code for resistance with respect to number of Layer.

```
q=1.602e-19;

h=6.626e-34;
Nch=1;
Nlayer=0:1:10;
R=(h/(2*q^2))./(Nch.*Nlayer);
plot(Nlayer,R);
xlabel('Number of layer');
ylabel('Resistance of GNR');
fid = fopen('Nlayer.doc','w');
fprintf(fid,'%10.10f\n',R);
fclose(fid);
```

4. MATLAB code for Inductance with respect to number of layer.

```
q=1.602e-19;
vf=8e5;
h=6.626e-34;
Nch=1;
Nlayer=0:0.1:4;
Lk=((h./(4*q^2).*vf)./(Nch.*Nlayer));
plot(Nlayer,Lk);
xlabel('Number of layer');
ylabel('Inductance');
fid = fopen('Nlayer.doc','w');
fprintf(fid,'%10.10f\n',Lk);
fclose(fid);
```

5. MATLAB code for Capacitance with respect to number of layer.

```
q=1.602e-19;
vf=8e5;
h=6.626e-34;
Nch=1;
Nlayer=0:1:4;
```

```
C=((Nch.*Nlayer).*((4*q^2)./(h*vf)));
plot(Nlayer,C);
xlabel('Nlayer');
ylabel('Capacitance');
C=C.*1e6;

fid = fopen('Nlayer.doc','w');
fprintf(fid,'%10.10f\n',Nlayer);
fclose(fid);
fid = fopen('capacitance.doc','w');
fprintf(fid,'%10.10f\n',C);
fclose(fid);
```